I&EC research
Industrial & Engineering Chemistry Research

pubs.acs.org/IECR
Article

Design of Storage Equipment for Unstable Chemicals Using Sensitivity-Based Methods

Published as part of Industrial & Engineering Chemistry Research special issue "Celebrating Undergraduate Research in Chemical Engineering 2024".

Giuseppe Andriani, Paolo Mocellin,* Gianmaria Pio, Ernesto Salzano, and Chiara Vianello

Cite This: *Ind. Eng. Chem. Res.* 2025, 64, 9529−9541
Read Online

ABSTRACT: The storage of thermally unstable chemicals poses significant risks, including runaway reactions that can lead to severe accidents. Developing inherently safe and cost-effective design strategies for storage vessels is essential for improving chemical plant safety and reliability. This study presents an advanced methodology based on an expanded Frank−Kamenetskii theory of self-heating (FKT), incorporating finite activation energy effects and mass consumption to address key limitations of the original framework. The approach integrates parametric sensitivity analysis to generate stability and performance diagrams, providing insights into safe and runaway operating regimes and optimizing storage policies. The methodology is validated using hydroxylamine-based systems, demonstrating its applicability to real-world cases. Experimental results show that a 30% w/w aqueous hydroxylamine solution can be stored at 35 °C in a vessel over twice the size required for a 50% solution. Sensitivity analyses reveal that the design outcomes are most influenced by the dimensionless heat of reaction and reaction order, with minimal dependence on the Lewis number. Refined FKT versions support the design of safer, larger vessels with characteristic sizes reduced by 10% compared to the original framework. However, increased refinement adds complexity. Therefore, applying different FKT versions at various design stages is recommended to balance accuracy and complexity.

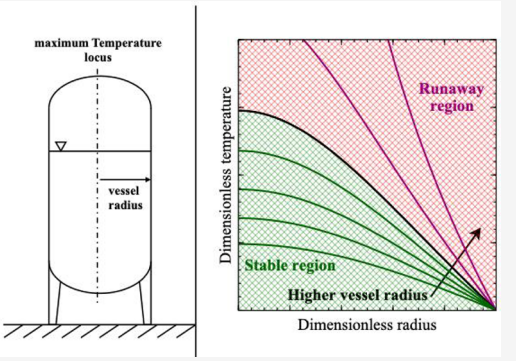

1. INTRODUCTION

Runaway phenomena are a major contributor to catastrophic industrial accidents involving reactive systems.[1] Effectively addressing these hazards necessitates the establishment of quantitative criteria to evaluate, manage, and mitigate the risks associated with exothermic reactions.[2] These measures are critical not only during the initial design stages of industrial equipment but also throughout ongoing operational processes.[3] Current safety protocols emphasize the design[4] and operational strategies[5] of chemical reactors to prevent uncontrolled exothermic reactions. However, significant risks also arise from improper chemical storage, where self-heating phenomena can escalate into hazardous scenarios if not properly managed.[6] In such cases, relief systems designed to vent decomposition products may prove inadequate.[7] Ensuring process safety under these conditions often depends solely on adhering to best practices during the design phase.[8,9]

Exothermic thermal decomposition is a prevalent and hazardous process encountered in the handling of unstable materials.[10] Comprehensive analysis of decomposition dynamics relies heavily on calorimetric studies, which remain a fundamental approach in this field.[11] These studies enable the determination of critical characteristics of thermal degradation reactions, including thermodynamic and kinetic properties, as well as onset and peak reaction parameters.[12] Commonly employed techniques include differential scanning calorimetry (DSC),[13] thermogravimetric analysis (TGA),[14] isothermal calorimetry,[15] adiabatic calorimetry,[16] reaction calorimetry,[17] and accelerating rate calorimetry (ARC).[18]

While calorimetric analysis provides reliable data on decomposition reactions,[19] the Frank−Kamenetskii theory of self-heating (FKT) serves as a valuable theoretical framework for understanding these phenomena and mitigating their risks.[20] The theory establishes practical criteria for evaluating the ability of storage vessel designs to dissipate thermal energy generated by unintended exothermic reactions.[21] FKT's numerical formulation assumes a quiescent fluid,[22] negligible wall thermal resistance ($Bi \to \infty$)[23] and conversion ($\chi \to 0$),[24] and nearly infinite dimensionless activation energy, i.e., $\gamma = E_a/$

Received: January 9, 2025
Revised: April 19, 2025
Accepted: April 22, 2025
Published: May 2, 2025

https://doi.org/10.1021/acs.iecr.5c00127
Ind. Eng. Chem. Res. 2025, 64, 9529−9541

$(R_gT_{amb}) \rightarrow \infty$.[25] For static conductive fluids, the assumption of $Bi \rightarrow \infty$ is typically valid without compromising model accuracy. However, extending FKT's applicability requires addressing the effects of γ and reactant consumption on the critical Frank−Kamenetskii number (δ_{crit}), which guides vessel design, and the maximum temperature (T_{max}) reached during storage. These refinements aim to improve the reliability and precision of design strategies for managing thermal risks.

To address the limitations in the applicability of the FKT, extending the theory is strongly encouraged. A robust analytical framework is needed to facilitate these advancements.[26] Building on the observation that δ_{crit} represents a metastable threshold beyond which steady-state solutions become unattainable due to runaway phenomena,[27] the Varma, Morbidelli, and Wu theory of parametric sensitivity analysis (VMWT) offers a promising approach.[28] This analysis aligns with the principles of bifurcation theory as applied to chemically reactive systems.[29] The VMWT provides practical tools for design, optimization, and control, including stability and performance diagrams. Depending on the required level of detail for a specific application, the VMWT can be applied to various representative models of reactive storage equipment, resulting in different parametric and bifurcation maps. An example in the literature demonstrates the combination of sensitivity analysis with the FKT to produce $\delta-\gamma$ stability diagrams and $\Theta_{max}-\gamma$ performance diagrams.[9] This approach involves relaxing the canonical FKT assumption of infinite activation energy, thereby expanding the theory's applicability to more realistic scenarios.

The FKT provides a robust framework for evaluating the intrinsic stability of chemical mixtures by integrating kinetic, thermodynamic, onset, and transport properties into a unified metric.[30,31] Assessing decomposition characteristics requires determining these parameters through experimental or theoretical approaches, each offering insights into distinct aspects of the reaction. For example, kinetic and onset data indicate the likelihood of reaction initiation, while reaction enthalpy quantifies the severity of the associated exothermic phenomena.[32] Traditional risk assessments typically combine probability and magnitude indices into a single indicator,[33] which is then compared to a user-defined scale to yield a qualitative risk classification.[34] Alternatively, relative comparisons between scenarios can be performed without relying on an external scale, enabling the identification of less hazardous alternatives.[35] However, a comprehensive protocol for intrinsic safety assessment that systematically incorporates all relevant data is still lacking in the literature. Existing indices are often based on technical definitions lacking a direct physical foundation and fail to account for equipment-specific heat dissipation mechanisms. Many evaluations assume adiabatic conditions, which are suitable for accident scenarios but less representative of standard operational conditions. Moreover, established methodologies frequently assess the likelihood and magnitude of runaway reactions separately before combining them into an overall risk level, potentially overlooking the dynamic interactions between these factors.

This study explores the integration of experimental data acquisition and numerical modeling to improve safety in chemical processes.[36] The proposed methodology is grounded in the principles of the inherently safer design (ISD),[37] with the primary goal of mitigating self-heating risks during the storage of thermally unstable substances.[38] By adopting this approach, the likelihood of runaway reactions is significantly reduced.[39]

In addition, the FKT addresses the limitations of traditional stability assessment methodologies by providing a quantitative, theory-based approach. Key parameters, such as the critical vessel radius $r_{w,crit}$ and the maximum temperature reached T_{max}, offer an integrated measure of a mixture's stability by combining kinetic, thermodynamic, transport, and onset information.[40] Higher $r_{w,crit}$ values indicate greater intrinsic stability, reflecting the system's capacity to store larger quantities safely without triggering runaway reactions. The condition $T_{max} < T_{onset}$ (where T_{onset} represents the onset temperature) further confirms the robustness of the assessment, ensuring that the predicted stability aligns with observed thermal behavior.

A case study is presented involving a 50% w/w aqueous solution of hydroxylamine (HA50), a compound commonly used in various chemical processes[41] and often combined with H_2O_2 to generate hydroxyl radicals.[42] Storage vessel designs are evaluated using three models: the classical FKT formulation, an extended version that incorporates the dependence of δ_{crit} on γ, and a comprehensive model that integrates the mass balance equation. The numerical outcomes of these approaches are compared, emphasizing how different modeling assumptions affect the reliability of design conclusions. The construction of stability and performance diagrams is also discussed, with a focus on the impact of incorporating the mass balance equation on previous design considerations. These diagrams offer valuable insights for optimizing storage strategies and ensuring the safe handling of reactive substances. Additionally, the behavior of the HA50 solution is compared with that of a more diluted 30% w/w aqueous hydroxylamine solution (HA30) to further validate the reliability and applicability of the FKT framework for stability comparisons of mixtures. This comparative analysis supports data-driven decision-making for full-scale industrial applications, demonstrating the utility of the FKT in guiding the safe and efficient design of storage systems.

This study builds upon a previous work by introducing key advancements that enhance the model's accuracy and applicability. A prior study[9] refined the original FKT model by considering the impact of finite activation energies. However, it did not incorporate the effects of reactant consumption due to the exothermic side reaction, which can play a crucial role in reactive storage scenarios. In this work, the model has been further developed by integrating mass balances, leading to a more comprehensive description of self-heating phenomena. This extension enhances the predictive capabilities of the framework while also introducing additional parameters that may influence the reliability of the results. Consequently, this study aims to explore the refined FKT formulation in greater depth, offering new insights into the role of these parameters in the stability and design of storage vessels. Furthermore, the case-study application is designed to facilitate the reproducibility of the methodology and provide a clearer understanding of its practical implications.

2. METHODOLOGY

This section outlines the methodology employed in this work. Section 2.1 identifies the key parameters required for analysis, which can be obtained experimentally or through a detailed literature review. This data set includes kinetic, onset, and physicochemical properties essential for the evaluation.

https://doi.org/10.1021/acs.iecr.5c00127
Ind. Eng. Chem. Res. 2025, 64, 9529−9541

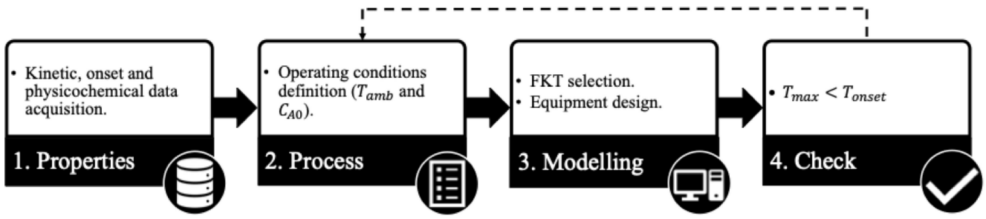

Figure 1. Flowchart illustrating the proposed methodological protocol. The dashed line represents the iterative loop, which adjusts the process conditions (Step 2) if the verification step (Step 4) is not satisfied.

Section 2.2 presents the storage vessel design framework, structured as follows: the canonical approach (Section 2.2.1), the first-order approximation (Section 2.2.2), and the second-order FKT formulation (Section 2.2.3). These models, all based on the Frank−Kamenetskii theory (FKT) of self-heating, are used to assess runaway phenomena caused by unintended temperature increases in solids or quiescent mixtures. Given the simplifications inherent in the classical FKT model, a parametric sensitivity analysis (Section 2.2.4) is introduced to refine the theoretical framework. The complete design protocol (Section 2.2.5) is then formulated, aiming to address gaps in the technical and scientific literature regarding the intrinsic safe sizing of storage vessels containing materials prone to exothermic side reactions.

The methodology is applied to a case study (Section 2.3), where the proposed strategies are evaluated and compared. This case study also provides a broader perspective on the instability of hydroxylamine-based solutions, employing a scientifically grounded approach that relies on two key metrics: the critical vessel radius ($r_{w,crit}$) and the maximum temperature reached (T_{max}).

Figure 1 provides a schematic overview of the proposed methodology.

2.1. Input Data. The first step of the proposed protocol focuses on identifying the key physicochemical data necessary for practical implementation. These critical parameters include:

- Kinetic data: activation energy (E_a), Arrhenius pre-exponential factor ($k_{k\infty}$), reaction rate expression, reaction order (n), initial concentration of the primary reactant (C_{A0}), a reaction enthalpy per mole ($\Delta\tilde{H}_r$).
- Onset characteristics: the onset temperature (T_{onset}) of the decomposition reaction, which serves as a key indicator of the material's thermal stability.
- Physicochemical properties: mixture's molar heat capacity ($\tilde{C}_p$), density (ρ), thermal conductivity (k_T) and mass diffusivity of the primary reactant in the stored mixture ($\mathcal{D}_{A,mix}$).

These parameters are essential for modeling decomposition reactions in hypothetical mixtures and provide the foundation for designing and sizing storage vessels based on the FKT. This requirement applies regardless of whether the classical or extended formulation of the theory is used.

2.2. Storage Vessel Design. The strategies for storage vessel sizing presented in this work are based on the Frank−Kamenetskii theory (FKT). To address the limitations related to the assumptions of the FKT theory, three distinct sizing approaches are proposed and analyzed in the present work:

- Canonical FKT Formulation: this baseline approach applies the classical FKT assumptions, serving as a reference point for further refinements.
- Extended FKT (relaxation of $\gamma \to \infty$ assumption): this approach relaxes the assumption of infinite dimensionless activation energy ($\gamma \to \infty$), enabling the calculation of more accurate critical Frank−Kamenetskii numbers (δ_{crit}) and maximum temperatures (T_{max}) for specific γ values.
- Comprehensive FKT model: the most advanced approach eliminates both the $\gamma \to \infty$ and $\chi \to 0$ assumptions. By incorporating coupled mass and energy balances, this model accounts for the depletion of reactants over storage time, yielding more realistic estimates for δ_{crit} and T_{max}.

The comprehensive model offers additional insights by linking thermal stability to the dynamics of reactant consumption during storage. This integration supports the development of optimal storage practices that not only enhance the safety and reliability of vessel designs but also minimize economic losses due to material degradation.

2.2.1. Canonical FKT Formulation. The conventional FKT assumes that a stationary fluid dissipates heat to its surroundings solely through conduction.[43] Under the condition Bi $\to \infty$, the ambient temperature is considered uniform and constant, while a temperature gradient forms within the system, with the maximum temperature of the reactive material occurring at the center of the vessel.[44] The governing equation of FKT, expressed in eq 1,[45] is derived under the assumption that the dimensionless temperature depends only on time and radial coordinates, reflecting the idealized cylindrical geometry of the system. This formulation determines the critical vessel radius ($r_{w,crit}$), beyond which runaway conditions may be triggered by self-heating. Additional assumptions of the FKT include negligible reactant conversion and infinitely high activation energy, leading to a conservative design approach for storage vessels susceptible to unintended decomposition reactions. Within this framework, the stored fluid is treated as nearly quiescent, with natural convective motion aiding heat dissipation from exothermic decomposition reactions. These idealized conditions prioritize safety, ensuring robust storage vessel designs while acknowledging the limitations of the model. The reaction rate is modeled as a unimolecular process.

$$r_{w,crit} = \sqrt{\frac{\delta_{crit} k_T R_g T_{amb}^2}{(-\Delta\tilde{H}_r) k_{k\infty} \exp\left(-\frac{E_a}{R_g T_{amb}}\right) C_{A0}^n E_a}} \quad (1)$$

In Equation 1, $r_{w,crit}$ denotes the critical vessel radius, δ_{crit} is the critical Franz−Kamenetskii number, k_T represents the mixture's thermal conductivity, R_g is the universal gas constant, T_{amb} is the reference ambient temperature, $\Delta\tilde{H}_r$ is the enthalpy

https://doi.org/10.1021/acs.iecr.5c00127
Ind. Eng. Chem. Res. 2025, 64, 9529−9541

of reaction per unit mole, $k_{k\infty}$ is the Arrhenius pre-exponential factor, E_a is the activation energy, C_{A0} is the initial concentration of the unstable substance and n is the reaction order.

δ_{crit} is strongly influenced by the system geometry[46,47] and for a cylindrical configuration,[48] $\delta_{crit} = 2$. Since the storage vessel is modeled as a cylinder, its characteristic dimension corresponds to the radius of the equipment. It is worth mentioning that different geometries can also be considered, as they influence the choice of the δ_{crit} value. In other words, by selecting an appropriate δ_{crit}, the methodology accounts for system shapes beyond the cylindrical configuration. A detailed list of δ_{crit} values for various geometries can be found in 44.

With a selected T_{amb}, $r_{w,crit}$ can be calculated, or conversely, an appropriate T_{amb} can be determined for a given radius. While quantitative details are provided in Section 3, key considerations for selecting T_{amb} are outlined here.

As shown in Equation 1, T_{amb} appears in both the numerator and denominator of the expression for $r_{w,crit}$. The quadratic dependence in the numerator is outweighed by the exponential dependence in the denominator, leading to a strong inverse correlation between T_{amb} and $r_{w,crit}$. As a result, small variations in T_{amb} can significantly impact the critical vessel radius. To account for temperature fluctuations, it is advisable to select the highest expected ambient temperature at the plant site. This ensures a conservative design, minimizing $r_{w,crit}$ and enhancing heat dissipation efficiency to reduce the risk of runaway conditions.

The physical interpretation of $r_{w,crit}$ lies in the system's capacity to manage self-heating phenomena. If $r > r_{w,crit}$, thermal energy dissipation becomes inadequate, potentially leading to a runaway reaction. Conversely, when $r \leq r_{w,crit}$, the material can be stored safely. It is crucial that the maximum temperature (T_{max}) remains below the decomposition onset temperature (T_{onset}). T_{max} is calculated using Equation 2, where the maximum dimensionless temperature for a cylindrical geometry[49] is $\Theta_{max} = \ln 4$.

$$T_{amb} + \frac{R_g T_{amb}^2}{E_a}\Theta_{max} \tag{2}$$

2.2.2. Extended FKT (Relaxation of $\gamma \to \infty$ Assumption). The first refinement of the classic FKT incorporates the influence of the dimensionless activation energy (γ) on the critical Frank−Kamenetskii number (δ_{crit}) and maximum dimensionless temperature (Θ_{max}).[9] This enhancement expands the set of design and validation parameters, increasing the robustness of the protocol and providing a deeper understanding of the effects of relaxing the $\gamma \to \infty$ assumption on numerical results. To account for these effects, the dimensionless one-dimensional heat balance equation in cylindrical coordinates is formulated as shown in Equation 3. This equation incorporates various dimensionless parameters, including dimensionless time $\mathcal{T} = t\alpha/r_w^2$ and dimensionless radial coordinate $\Omega = r/r_w$, as well as additional parameters defined in Equation 4 and Equation 5.

The reaction rate is modeled as a unimolecular process, proportional to the reactant concentration raised to a generic exponent n. For simplicity and completeness, a single unimolecular reaction ($A \to$ products) is considered to represent a single decomposition mechanism.

$$\frac{\partial\Theta}{\partial\mathcal{T}} = \frac{\partial^2\Theta}{\partial\Omega^2} + \frac{1}{\Omega}\frac{\partial\Theta}{\partial\Omega} + \delta\exp\left(\frac{\Theta}{1+\Theta/\gamma}\right) \tag{3}$$

$$\Theta = \gamma\frac{T - T_{amb}}{T_{amb}} \tag{4}$$

$$\delta = \frac{\gamma(-\Delta\tilde{H}_r)\mathcal{R}|_{T_{amb},C_{A0}}r_w^2}{k_T T_{amb}} \tag{5}$$

The boundary conditions for the system assume symmetry at the center of the reactive mass and thermal equilibrium with ambient conditions at the external surface of the storage vessel. As the initial condition, the temperature of the reactive mass is assumed to be uniform and equal to the ambient temperature.

2.2.3. Comprehensive FKT Model. The second refinement of the FKT removes the simplifying assumptions of both $\gamma \to \infty$ and $\chi \to 0$. To accomplish this, the transient, dimensionless mass and heat balance equations are introduced, as shown in Equation 6 and Equation 7, respectively. These equations incorporate additional dimensionless parameters, including the Lewis number ($Le = /\mathcal{D}_{A,mix}$), the normalized concentration of the reactant ($u_A = C_A/C_{A0}$) and the dimensionless heat of reaction B (Equation 8). The reaction rate corresponds to a unimolecular process.

$$\frac{\partial\Theta}{\partial\mathcal{T}} = \frac{\partial^2\Theta}{\partial\Omega^2} + \frac{1}{\Omega}\frac{\partial\Theta}{\partial\Omega} + \delta u_A^n\exp\left(\frac{\Theta}{1+\Theta/\gamma}\right) \tag{6}$$

$$\frac{\partial u_A}{\partial\mathcal{T}} = \frac{1}{Le}\left(\frac{\partial^2 u_A}{\partial\Omega^2} + \frac{1}{\Omega}\frac{\partial u_A}{\partial\Omega}\right) + \frac{B}{\delta}\nu_A u_A^n\exp\left(\frac{\Theta}{1+\Theta/\gamma}\right) \tag{7}$$

$$B = \gamma\frac{(-\Delta\tilde{H}_r)C_{A0}}{\rho\hat{C}_p T_{amb}} \tag{8}$$

Similarly to Section 2.2.2, The boundary and initial conditions are extended to include both energy and mass balances. At the center of the reactive system ($\Omega \to 0$), symmetry is invoked, resulting in zero gradients for both temperature and concentration. At the external boundary of the system ($\Omega \to 1$), thermal equilibrium with the ambient environment is assumed, ensuring that the external temperature remains equal to T_{amb}. Additionally, for the mass balance at the boundary, negligible reactant flux is considered, reflecting the assumption that reactant diffusion is minimal at this location. For the initial conditions, the reactive mass temperature is set equal to the ambient temperature at $\mathcal{T} \to 0$, while the initial concentration of the stored material corresponds to an imposed reference value C_{A0}.

2.2.4. Sensitivity Analysis. To ensure both high safety standards and optimal performance during the design, optimization and control of storage vessels handling materials prone to exothermic reactions, the VMWT provides a well-established framework.[50,51] Implementing sensitivity analysis for reactive systems involves identifying an observable that reflects how the system's behavior changes in response to variations in design or operational parameters.[52,53] Given the focus on preventing runaway reactions, it is standard practice to select $S(\Theta;B)$—the normalized sensitivity of the Θ with respect to B—as the key observable. The formulation of $S(\Theta;B)$ is presented in Equation 9.

https://doi.org/10.1021/acs.iecr.5c00127
Ind. Eng. Chem. Res. 2025, 64, 9529−9541

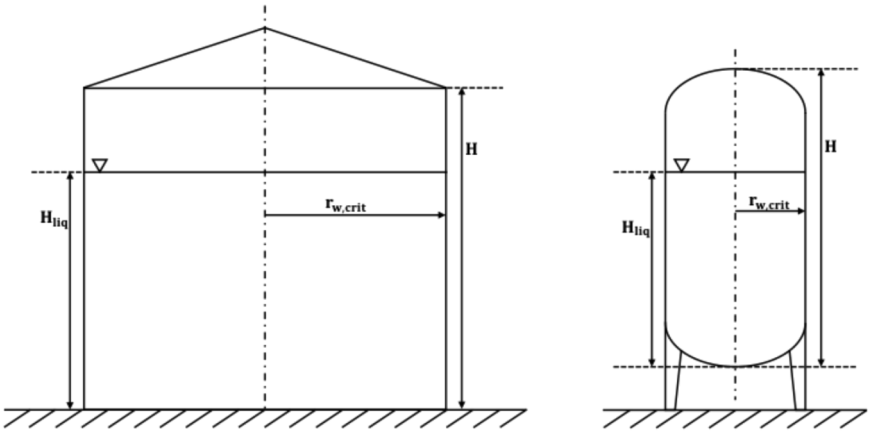

Figure 2. Schematic representation of two storage vessel configurations: the left illustrates a design for larger volumes of stored liquid, while the right represents a configuration for smaller quantities.

$$S(\Theta;\, B) = \frac{B}{\Theta}\frac{\partial\Theta}{\partial B} \tag{9}$$

Examining the relationship described in Equation 9, it becomes evident that when $S(\Theta;B)$ reaches its peak, the equipment transitions from a stable and controlled operational regime to a runaway condition.[54] It is, therefore, essential to pinpoint the conditions under which this bifurcation occurs to prevent it, allowing for adjustments in system design and operational parameters to ensure both safety and efficiency.[55]

It is worth noting that B does not appear explicitly in all the equations reported in previous sections. For this reason, it is proposed to involve as observable the normalized sensitivity of Θ with respect to δ for the analysis of storage vessels, to have a unified representation of the bifurcation analysis (Equation 10).

$$S(\Theta;\, \delta) = \frac{\delta}{\Theta}\frac{\partial\Theta}{\partial\delta} \tag{10}$$

Due to the generality of the sensitivity criterion of the VMWT, the use of $S(\Theta;\delta)$ can still be considered as legitimate, and appropriate to identify stable to unstable regimes transitions properly. To do so, the reference constitutive systems equations must be solved in conjunction with the corresponding set of sensitivity equations, obtained by direct differentiation of the balances with respect to δ, along with the associated boundary and initial conditions.[56]

Eventually, the results obtainable with the sensitivity analysis can be synthesized in a stability and performance bidimensional diagrams. The former, synthesize the working regimes of the systems in a parametric diagram, together with the locus of values under which the transition from a stable to an unstable behavior will occur. The latter, reports the trend of system dependent variable (or a quantity directly related to that) in a bifurcation diagram. In this way, the observable behavior of the system under the transitional limit from one regime to another can be summarized.

2.2.5. Design Algorithm. The results of the sizing methodology are expressed in terms of $r_{w,crit}$, i.e., the critical radius for preventing runaway reactions caused by self-heating. This parameter represents a metastable threshold: when $r > r_{w,crit}$, the system is unable to dissipate the heat generated by unintended exothermic reactions, leading to runaway conditions. Conversely, for $r \leq r_{w,crit}$, the material can be safely stored and managed. Thus, $r_{w,crit}$ is a key geometric design variable that must be carefully evaluated to ensure safe and reliable storage operations. The critical radius $r_{w,crit}$ is calculated using Equation 1. Its validity is confirmed by comparing T_{max}, obtained from Equation 2, with the onset temperature T_{onset} from calorimetric experiments. The condition $T_{max} < T_{onset}$ ensures that the calculated $r_{w,crit}$ value corresponds to an intrinsically safe design.

Calculating $r_{w,crit}$ using Equation 1 and Equation 2 requires prior knowledge of δ_{crit} and Θ_{max}. According to the standard FKT and in cylindrical systems, $\delta_{crit} = 2$ and $\Theta_{max} = \ln 4$. In the extended FKT, δ_{crit} and Θ_{max} depend on γ, requiring sensitivity analysis to determine their values. In the comprehensive FKT formulation, these parameters also depend on Le and B.

The advantages of more refined FKT models are justified by their reduced modeling assumptions, resulting in more realistic δ_{crit} and Θ_{max} values. By closely reflecting actual system behavior, these refined models support more precise and economically competitive equipment designs while allowing a detailed analysis of how assumptions affect numerical outcomes. This analysis is crucial for bridging theoretical methods with full-scale industrial applications. In early conceptual and basic design phases, less resource-intensive FKT versions—such as the fundamental or expanded FKT—are often sufficient. However, in advanced design and optimization steps, the comprehensive FKT provides a more accurate basis for defining the final equipment configuration. During iterative design, where multiple configurations are proposed, simpler models help manage complexity. Conversely, once the reference configuration is outlined, refined models guide the final design more precisely, optimizing resource allocation.

For completeness, after calculating and verifying $r_{w,crit}$, reference manuals such as API guidelines,[57] should be consulted to finalize the overall storage vessel design. While $r_{w,crit}$ defines the radial dimension of the vessel, the height and degree of filling must also be determined. Unlike the critical radius, these variables depend on operational, mechanical, and site-specific considerations rather than heat management constraints.

2.3. Case Study. To demonstrate the application of the proposed methodology, a case study was conducted involving a 50% w/w aqueous solution of hydroxylamine (HA50), a material prone to violent decomposition. At this concentration, HA50 poses a significant risk of detonation.[41] The reaction kinetics, thermodynamic properties, and onset temperatures

https://doi.org/10.1021/acs.iecr.5c00127
Ind. Eng. Chem. Res. 2025, 64, 9529−9541

for HA50 are well-documented,[40] while additional correlations and numerical values were sourced from established references [58, 59]. Experimental data were obtained using a thermal screening unit (TSu) calorimeter, which facilitates accelerating rate calorimetry (ARC) tests.[60]

For this study, the ambient temperature was assumed to be equal to the wall temperature, consistent with the assumption of negligible thermal resistance at the wall. Three ambient temperatures were evaluated—5 °C, 20 °C, and 35 °C—to represent realistic annual environmental conditions. The system geometry was modeled as a vertically oriented cylindrical storage vessel. Figure 2 illustrates two possible storage vessel configurations: the left for larger volumes and the right for smaller quantities of the unstable liquid. The total equipment height and liquid fill level must be determined according to specific standards and regulations.

The methodology can also be applied to horizontal cylindrical vessels, provided that appropriate norms are followed to determine the length of the vessel once $r_{w,crit}$ is calculated. In this case, the vertical setup was preferred to optimize the plant's surface area utilization.

To further demonstrate the applicability of the FKT in assessing the intrinsic stability of unstable mixtures, aqueous hydroxylamine solutions of different concentrations (30% w/w − HA30 − and 50% w/w − HA50) were analyzed. By applying the canonical, extended, and comprehensive FKT formulations, the influence of modeling assumptions on safety assessment protocols was explored. Calculations of $r_{w,crit}$ and T_{max} were performed using kinetic, thermodynamic, and onset data from the literature[40,58,59] under varying ambient temperatures (5 °C, 20 °C, and 35 °C), representing cold, temperate, and hot environments.

3. RESULTS AND DISCUSSIONS

Section 3.1 discusses the stability and performance of the reactive system using the proposed FKT versions. This section lays the groundwork for understanding system behavior, enhancing the accuracy of the design algorithm. The case study results are provided in Section 3.2.

Section 3.1.1 examines the effect of the dimensionless heat of reaction (B), while Sections 3.1.2 and 3.1.3 analyze the influence of the Lewis number (Le) and reaction order (n).

3.1. General Stability and Performance Considerations. This section explores the impact of modeling assumptions on sensitivity analysis results, using the VMWT approach to summarize system behavior in two key representations: stability diagrams ($\delta-\gamma$) and performance diagrams ($\Theta_{max}-\gamma$). A detailed analysis of how variations in governing parameters influence these diagrams is provided. In the realm of storage vessels analyses containing unstable substances, the stability diagram should show the trend of δ_{crit} on the y-axis as a function of another system governing parameter variation. On the other hand, the performance diagram should report the dependence of Θ_{max} determined at δ_{crit} and as a function of the same parameter reported on the stability diagram x-axis.

3.1.1. Effect of the Dimensionless Heat of Reaction (B). The first parameter examined is the dimensionless heat of reaction (B). The corresponding diagrams delineate two distinct operating regimes: stable and runaway. To ensure a comprehensive analysis, the results obtained using the standard FKT formulation, as well as the two expanded versions, are included. Figures 3 and 4 present the stability and performance diagrams generated for various B.

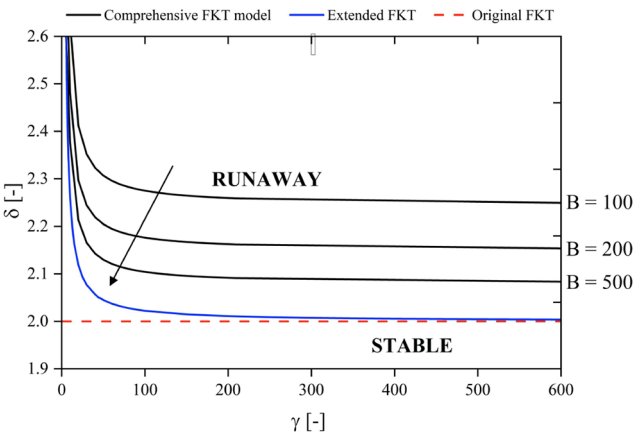

Figure 3. Stability diagram obtained varying the dimensionless heat of reaction B (for Le = 100 and n = 1). Results are compared with the reference value δ_{crit} = 2 of the canonical FKT formulation, represented by the red dashed line. The arrow indicates increasing value of B.

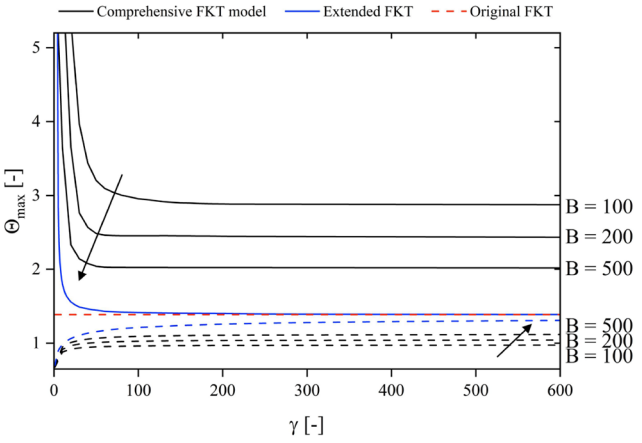

Figure 4. Performance diagram obtained varying dimensionless heat of reaction B (for Le = 100 and n = 1). Solid lines represent Θ_{max} values determined at $\delta = \delta_{crit}$, while dashed lines correspond to Θ_{max} at δ = 2. Results are compared with the reference value Θ_{max} = ln 4 of the canonical FKT formulation represented by the red dashed line. The arrows indicate increasing value of B.

Analyzing Figure 3, it is clear that the runaway region expands with increasing B. This behavior is expected, as higher B values indicate that the chemical reactions generate greater thermal energy per mole of reactant consumed. As a result, the risk of thermal runaway due to self-heating phenomena rises with the dimensionless heat of reaction. In these conditions, the critical metastable values of δ, beyond which self-heating leads to runaway, decrease. When δ exceeds this critical threshold, safe storage can no longer be ensured, and the system's temperature profile will diverge uncontrollably, making thermal management and system stability impossible. Eventually, for B > 1000 practically no differences can be retrieved between the expanded and comprehensive models, since both theories predicts practically the same δ_{crit} (i.e., the black and blue solid curves practically are overlapped).

From a design perspective, higher δ values necessitate larger storage vessels to safely accommodate unstable substances, as

https://doi.org/10.1021/acs.iecr.5c00127
Ind. Eng. Chem. Res. 2025, 64, 9529−9541

indicated by Equation 1. Increasing the vessel size, while maintaining a fixed height-to-diameter aspect ratio, optimizes plant footprint utilization and results in equipment designs that are more practical and industrially appealing.

The expanded FKT provides an asymptotic worst-case scenario relative to the second expanded formulation, offering a conservative yet reliable design option. Meanwhile, the original FKT, being the most conservative of the three models, facilitates the design of smaller vessels with enhanced safety margins. However, there is an inverse relationship between the complexity and conservativeness of the formulations: the original FKT is the simplest and most conservative, followed by the extended and then the comprehensive FKT formulations. This trade-off between complexity and conservativeness must be carefully considered when selecting the most appropriate model for a given application.

Turning to Figure 4, it is essential to note that it illustrates the maximum dimensionless temperature (Θ_{max}) reached at the stability-to-runaway transition limits. Solid lines represent bifurcation profiles derived using the extended and comprehensive FKT formulations at the δ values shown in Figure 3. Dashed lines, on the other hand, correspond to bifurcation profiles assuming a fixed $\delta = 2$. This comparison highlights the conservativeness of the Θ_{max} predictions by the canonical FKT, which assumes a constant critical $\delta = 2$ and a corresponding $\Theta_{max} = \ln 4$, as depicted in Figures 3 and 4. Examining the solid curves in Figure 3 reveals that the trend $\Theta_{max}(\gamma)$ parallels the $\delta-\gamma$ relationship in Figure 2. As B decreases, Θ_{max} for a constant γ decreases, reflecting a requirement for larger storage vessels due to lower δ.

Process equipment with a higher critical wall radius ($r_{w,crit}$) can safely accumulate more heat generated from self-heating without initiating runaway conditions. Consequently, higher internal dimensionless temperatures can be reached without compromising thermal control. The expanded FKT serves as an asymptotic limit of the more refined formulation, while the original FKT remains the most conservative option.

From a design perspective, Θ_{max} plays a critical role in verifying the proposed equipment configuration (Section 2.2.1). Selecting an appropriate Θ_{max} value ensures inherent safe equipment, particularly when employing less conservative but more refined FKT formulations. Alternatively, the original FKT offers a highly conservative and computationally straightforward approach to equipment sizing.

If the verification step using $\Theta_{max} = \ln 4$ is successful, it guarantees that the actual maximum temperatures will remain lower, further enhancing safety. As illustrated by the dashed curves in Figure 2, when $\delta = 2$, the internal equipment temperature remains below the level predicted by the original FKT. This outcome underscores the conservativeness of the standard FKT method, making it a reliable baseline for ensuring safe design.

3.1.2. Effect of the Lewis Number (Le). This section examines the impact of variations in the Lewis number (Le) on the stability and performance of storage vessels containing reactive materials. Similar to the approach in Section 3.1.1, the results are summarized using stability (Figure 5) and performance (Figure 6) diagrams.

Figure 5 illustrates the relationship between the Lewis number (Le) and the runaway region, which expands as Le decreases. This trend occurs because higher Le values indicate that thermal diffusivity dominates over mass diffusivity, improving the ability of the system to dissipate thermal

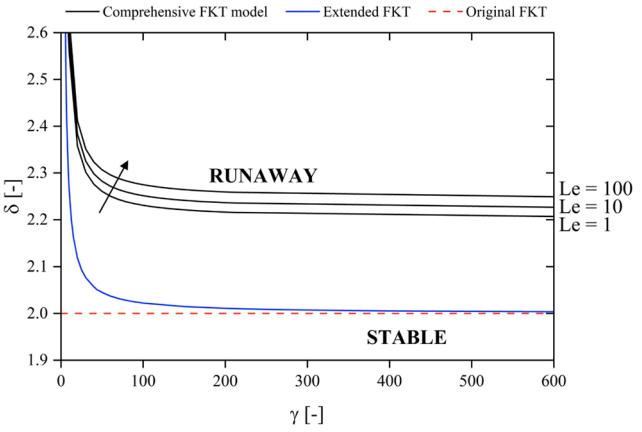

Figure 5. Stability diagram obtained varying the Lewis number Le (for $B = 100$ and $n = 1$). Results are compared with the reference value $\delta_{crit} = 2$ of the canonical FKT formulation represented by the red dashed line. The arrow indicates increasing value of Le.

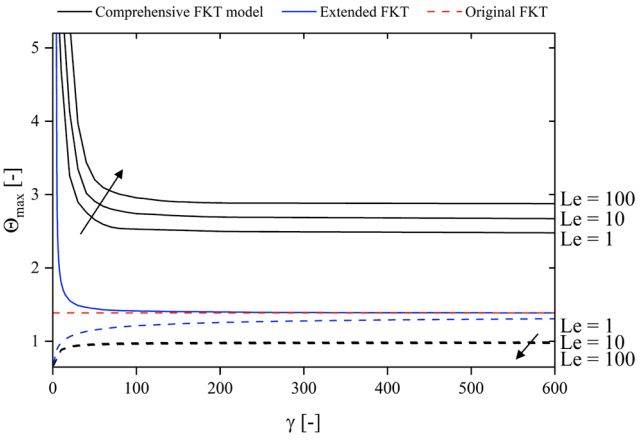

Figure 6. Performance diagram obtained varying the Lewis number Le (for $B = 100$ and $n = 1$). Solid lines represent Θ_{max} values determined at $\delta = \delta_{crit}$, while dashed lines correspond to Θ_{max} at $\delta = 2$. Results are compared with the reference value $\Theta_{max} = \ln 4$ of the canonical FKT formulation represented by the red dashed line. The arrow indicates increasing value of Le.

energy. Enhanced thermal energy dissipation mitigates self-heating effects, thereby reducing the risk of runaway. Consistent with previous analyses, the extended FKT formulation provides a conservative limit for stability and design purposes.

Comparing Figure 5 to Figure 3 reveals the system's differing sensitivities to variations in dimensionless parameters. In Figure 3, B ranges from 100 to 500, while in Figure 5, Le spans 3 orders of magnitude (1 to 100). Despite this larger relative variation in Le, the resulting enlargement of the runaway region is smaller than that caused by the 5-fold change in B. This suggests that the system is more sensitive to variations in B than in Le. Practically, this underscores the critical importance of accurate calorimetric measurements for parameters influencing B, including $\Delta\tilde{H}_r$ and E_a.

Focusing on the performance diagram in Figure 6, the transition between stable and runaway regimes can be analyzed further in terms of apparent system behavior. Similar to Section 3.1.1, Θ_{max} values corresponding to $\delta = 2$ (dashed lines) and $\delta = \delta_{crit}$ (solid lines) are reported. Higher δ_{crit} values correspond to larger equipment radii, allowing for increased

https://doi.org/10.1021/acs.iecr.5c00127
Ind. Eng. Chem. Res. 2025, 64, 9529−9541

thermal energy accumulation and higher internal temperatures. Conversely, designing a vessel with $\delta = 2$ results in a more conservative configuration, as the imposed value exceeds the actual critical threshold. This conservative approach ensures that the vessel dissipates heat more effectively than predicted by either the refined or less conservative FKT formulations, providing an additional safety margin due to the constraints imposed by the model assumptions.

3.1.3. Effect of the Reaction Order (n). The final parameter under analysis is the reaction order n. Similar to $\Delta\tilde{H}_r$, E_a and $k_{k\infty}$, the reaction order and rate expression are typically determined through data analysis of calorimetric experiments. In this context, examining the impact of n on overall stability and performance is of both theoretical and practical importance. From a theoretical perspective, this analysis completes the framework by exploring how variations in n influence system behavior. Practically, it highlights the potential consequences of inaccuracies in data interpretation on the design of reactive storage vessels. Understanding the sensitivity of design outcomes to errors in determining n is crucial for ensuring reliable and safe storage solutions. As in the previous sections, stability and performance diagrams are presented in Figures 7 and 8, offering a detailed visualization of the system's behavior under varying values of n.

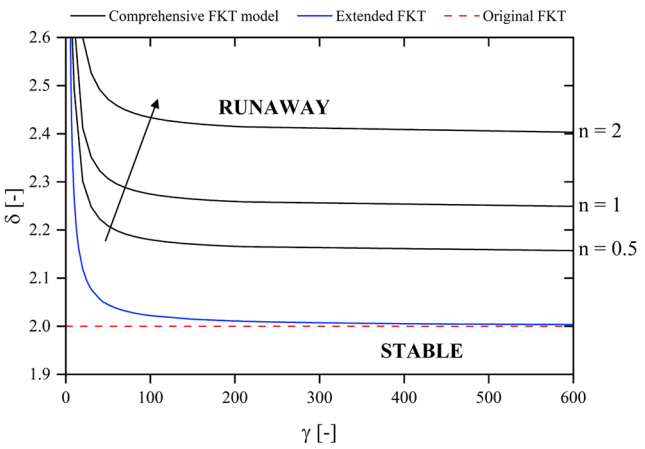

Figure 7. Stability diagram obtained varying the order of reaction n (for $B = 100$ and $Le = 1$). Results are compared with the reference value $\delta_{crit} = 2$ of the canonical FKT formulation represented by the red dashed line. The arrow indicates increasing value of n.

Examining the curves in Figure 7, it is evident that the stability region diminishes as the reaction order n decreases, gradually converging toward the results predicted by the expanded FKT and the original formulation. This behavior is driven by the interplay between mass and energy balances, which becomes increasingly pronounced with higher n. A higher reaction order strengthens the coupling between these balances, leading to greater reactant consumption as the reaction progresses. This suppresses the reaction rate, reducing thermal power generation and, consequently, the risk of runaway due to self-heating phenomena. The sensitivity of the stability-to-runaway transition boundary to variations in n can be further analyzed in light of Section 3.1.2. Errors in determining n significantly affect the prediction of system behavior, as evidenced by the marked differences observed across various n values. Comparing this sensitivity to that

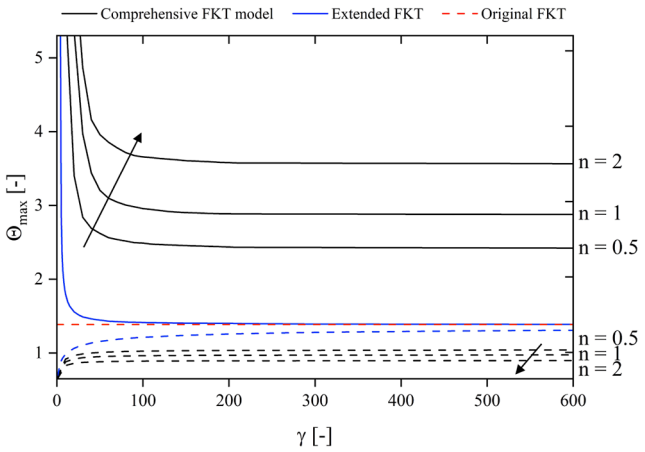

Figure 8. Performance diagram obtained varying the order of reaction n (for $B = 100$ and $Le = 1$). Solid lines represent Θ_{max} values determined at $\delta = \delta_{crit}$, while dashed lines correspond to Θ_{max} at $\delta = 2$. Results are compared with the reference value $\Theta_{max} = \ln 4$ of the canonical FKT formulation represented by the red dashed line. The arrow indicates increasing value of n.

observed for B (Figure 3) and Le (Figure 5), the system's sensitivity follows the order $B > n > Le$.

Turning to the performance diagram in Figure 8, the trends in Θ_{max} at δ_{crit} and $\delta = 2$ are clearly delineated. As in previous sections, the stability-to-runaway boundary shifts toward higher δ values in the stability diagram, causing the corresponding Θ_{max} to increase. For larger δ_{crit} values, the gap between the actual critical value and the assumed $\delta = 2$ widens. Consequently, the actual maximum temperature remains progressively lower than ln4, reflecting the conservative nature of the canonical FKT and its value in ensuring safety.

3.2. Design of the Storage Vessel. Building on the discussion of the intrinsic stability and performance characteristics of storage vessels containing reactive materials (Section 3.1), this section applies that knowledge to the design process considering storage systems for hydroxylamine at 50% w/w (HA50) and 30% w/w (HA30). The employed design methodology, detailed in Section 2.2.5, leverages the physicochemical parameters outlined in Section 2.3.

To simplify the analysis, the atmospheric, external, and internal vessel wall temperatures were assumed to be equal, consistent with the assumptions of $Bi \rightarrow \infty$ and negligible thermal resistance of the vessel walls. Under these conditions, variations in ambient temperature directly influence the vessel's thermal behavior. Table 1 summarizes the critical Frank−Kamenetskii parameters (δ_{crit}) and maximum dimensionless temperatures (Θ_{max}) corresponding to each ambient temperature (T_{amb}).

From the data presented in Table 1, it is evident that δ_{crit} increases across the different FKT formulations. When the influence of γ on δ_{crit} is incorporated in the FKT approach, the critical Frank−Kamenetskii number trends toward an asymptotic value of 2 (Figures 2, 4, and 6) as the dimensionless activation energy becomes large. This behavior is consistent with the foundational assumptions of the canonical FKT formulation. A similar trend is observed for Θ_{max}, which converges to the asymptotic value of 1.386 (ln 4) only at very high γ values (Figures 3, 5, and 7).

https://doi.org/10.1021/acs.iecr.5c00127
Ind. Eng. Chem. Res. 2025, 64, 9529−9541

Table 1. HA50 Storage System Critical Frank−Kamenetskii parameter (δ_{crit}) and maximum dimensionless temperature (Θ_{max}) as a function of the ambient temperature selected (T_{amb})

Hydroxylamine 50% w/w	Ambient temperature	Dimensionless activation energy	Lewis number	Dimensionless heat of reaction	Critical FK parameter	Max dimensionless temperature	
	T_{amb} [K]	γ [−]	Le [−]	B [−]	δ_{crit} [−]	$\Theta_{max}\|_{\delta_{crit}}$ [−]	$\Theta_{max}\|_{\delta=2}$ [−]
Canonical FKT	278.15	-	-	-	2.00	1.39	1.39
	293.15	-	-	-			
	308.15	-	-	-			
Extended FKT	278.15	44.50	-	-	2.05	1.44	1.14
	293.15	42.22	-	-	2.05	1.45	1.14
	308.15	40.17	-	-	2.06	1.45	1.14
Comprehensive FKT	278.15	44.50	70.51	69.40	2.40	3.24	0.91
	293.15	42.22	76.38	62.48	2.43	3.44	0.90
	308.15	40.17	81.66	56.54	2.47	3.97	0.89

Marked deviations between the original and extended FKT models occur at lower γ, emphasizing the necessity of more detailed formulations to address scenarios with low dimensionless activation energies. This asymptotic behavior is also apparent in the comprehensive FKT model (Figures 2−7) for both δ_{crit} and Θ_{max}. However, when the effects of B and Le are included, the predictions from the canonical FKT diverge significantly from those of the extended model, illustrating the increased computational effort required for more accurate design approaches.

Designing storage vessels based on $\delta = 2$ (as in the canonical FKT) results in a conservative design from two perspectives. First, the actual critical FK number determined by the extended and comprehensive FKT models is consistently higher, leading to smaller but more thermally efficient vessels. Second, the actual maximum temperature reached at $\delta = 2$ is always lower than that imposed by the canonical FKT.

From a methodological standpoint, if the verification step is satisfied for $\Theta_{max} = \ln 4$, it will also be satisfied at lower actual maximum temperatures. Conversely, to design the least conservative vessel size, the extended and comprehensive FKT models must be used, ensuring the correct Θ_{max} value is applied at $\delta = \delta_{crit}$ to avoid misleading and unsafe conclusions.

Once δ_{crit} and Θ_{max} are determined, the next step involves sizing and verifying the storage tank to ensure safe and efficient operation under the defined conditions.

The numerical results presented in Table 1 provide additional insights into the application of the three FKT formulations. Within the analyzed range of γ (from 40.17 to 44.50), the extended and canonical FKT yield nearly identical results for δ_{crit} and $\Theta_{max}|_{\delta_{crit}}$. The primary deviation is observed in $\Theta_{max}|_{\delta=2}$, highlighting the conservativeness of the canonical FKT in predicting the maximum temperature, a critical parameter for verification. When the effects of B, Le, and n are incorporated, larger deviations are observed in δ_{crit}, $\Theta_{max}|_{\delta_{crit}}$, and $\Theta_{max}|_{\delta=2}$. Higher δ_{crit} values lead to increased critical radii ($r_{w,crit}$), allowing for greater thermal energy accumulation. However, these higher radii also lead to increased $\Theta_{max}|_{\delta_{crit}}$, which may not satisfy verification criteria. As the fundamental assumptions of the canonical FKT are progressively relaxed, the disparity between the $\Theta_{max}|_{\delta=2}$ values predicted by the refined models and the canonical value grows. Results obtained from all three FKT formulations are summarized in Table 2 for ease of reference.

Table 2 highlights the significant influence of ambient temperature (T_{amb}) on the critical radius of the vessel ($r_{w,crit}$).

Table 2. HA50 Storage System Vessel design parameters as a function of the ambient temperature selected (T_{amb}). The onset temperature (T_{onset}) of the HA50 system is 393 K

Hydroxylamine 50% w/w	Ambient temperature T_{amb} [K]	Critical vessel radius $r_{w,crit}$[m]	Max temperature at δ_{crit} $T_{max}\|_{\delta_{crit}}$ [K]	Max temperature at $\delta = 2$ $T_{max}\|_{\delta=2}$ [K]
Canonical FKT	278.15	2.92	286.82	286.82
	293.15	1.02	302.77	302.77
	308.15	0.40	318.79	318.79
Extended FKT	278.15	2.96	287.15	285.30
	293.15	1.04	303.20	301.06
	308.15	0.41	319.30	316.86
Comprehensive FKT	278.15	3.21	298.38	283.85
	293.15	1.13	317.00	299.40
	308.15	0.45	338.57	314.97

As T_{amb} increases, the characteristic size of the storage vessel decreases significantly. This behavior aligns with predictions from both the original and expanded FKT models. To ensure robust safety measures in a hypothetical plant, it is crucial to analyze the temperature distribution over time and use the maximum observed value as the design reference. Relying on an average temperature, such as the midpoint between typical winter and summer conditions (5 and 35 °C), could lead to inaccurate conclusions and potentially unsafe designs.

Importantly, across all modeling approaches, the maximum temperature T_{max} remains well below the onset temperature T_{onset} (393 K). This ensures that the system operates safely, avoiding runaway conditions associated with the thermal decomposition of reactive materials.

Another key observation from Table 2 is the relationship between $r_{w,crit}$ and T_{max} based on the chosen approach. For a given T_{amb}, less conservative formulations yield larger critical radii and higher maximum temperatures. The comprehensive FKT model, in particular, supports the design of larger storage vessels, which are inherently safer due to their increased capacity to dissipate heat. However, ensuring safety requires rigorous validation of T_{max} against T_{onset}, especially when using less conservative formulations.

The strength of the FKT lies in its reliance on the well-established theory of thermal explosions, which eliminates subjective criteria and provides a physically meaningful interpretation of the results. Tables S1 and S2 summarize the dimensionless and dimensional parameters derived from

https://doi.org/10.1021/acs.iecr.5c00127
Ind. Eng. Chem. Res. 2025, 64, 9529−9541

the three FKT formulations and are reported in the Supporting Information.

For the diluted hydroxylamine mixture (HA30), as well as for the concentrated one (HA50), the extended and canonical formulations of the FKT predict nearly identical δ_{crit} values, with an average deviation of approximately 2.5% (see Table S1). This is mainly due to the value of dimensionless activation energy, approximatively equal to 40, threshold value above which the canonical and extended FKT practically predicts the same design values. Larger deviations are observed in the maximum dimensionless temperature at $\delta = 2$, with the canonical FKT overestimating by about 20%. This overestimation is on the conservative side, predicting a higher maximum temperature and thus establishing a more stringent verification criterion through the $T_{max} < T_{onset}$ condition.

The dimensional quantities in Table S2 confirm the strong dependence of results on ambient temperature. At higher T_{amb}, the $r_{w,crit}$ value is approximately 15% of the value predicted at lower ambient temperatures, underscoring the impact of thermal conditions on system stability. Using the comprehensive model, $r_{w,crit}$ increases by 10−15% under higher T_{amb}, while T_{max} rises proportionally by about 14%. This increase has implications for verification steps, as the gap between T_{max} and T_{onset} narrows, though the $T_{max} < T_{onset}$ criterion remains valid, confirming the design's robustness. In contrast, the canonical FKT predicts slightly lower T_{max} at $\delta = 2$, which further enhances safety by overestimating potential risks.

Comparing the results for the concentrated HA50 mixture (Tables 1 and 2) with the diluted HA30 mixture (Tables S1 and S2) from a stability perspective, HA30 exhibits greater resistance to decomposition compared to HA50. This is evident from the higher δ_{crit} and $r_{w,crit}$ values across all FKT formulations for HA30, indicating its capacity to be stored in larger equipment without triggering runaway conditions. At 35 °C, the critical radius $r_{w,crit}$ for HA30 is more than twice that of HA50, and the wider gap between T_{max} and T_{onset} further emphasizes its higher stability. These metrics enable a straightforward and integrated evaluation of intrinsic stability, combining factors including likelihood and severity into a single safety index, avoiding the need to assess kinetic, thermodynamic, and onset parameters individually.

From a design perspective, the ability to accommodate larger $r_{w,crit}$ values optimize plant footprints. For a fixed vessel geometry, higher $r_{w,crit}$ supports larger storage capacities, reducing the need for multiple storage units. However, the reduced hydroxylamine concentration in HA30 (0.6 times that of HA50) necessitates additional process units for concentration if higher tenors (e.g., 50% w/w) are required. This trade-off between long-term safety and operational costs highlights the decision-making challenges in selecting appropriate storage strategies.

Methodologically, the canonical, extended, and comprehensive FKT formulations demonstrate their utility across different design stages. The canonical FKT, with its predefined values ($\delta_{crit} = 2$ and $\Theta_{max} = \ln 4$), offers a simplified yet conservative approach suitable for preliminary equipment sizing. The extended FKT introduces greater sensitivity to activation energy variations by deriving specific δ_{crit} and Θ_{max} values from stability and performance diagrams, requiring only marginal additional effort. The comprehensive FKT, ideal for advanced design phases, accounts for input parameters like B, Le, n and γ using sensitivity analyses, allowing for a refined assessment of system behavior. This model can predict deviations of over 15% in $r_{w,crit}$ under the same T_{amb}, accompanied by stricter verification steps due to increased δ_{crit} and Θ_{max}. If verification fails, iterative adjustments to δ_{crit} and corresponding Θ_{max} values are required. Less refined FKT formulations provide a more straightforward methodology for both equipment design and stability assessment. Conversely, adopting more advanced formulations enables the design of less conservative equipment, optimizing economic feasibility and plant footprint utilization. A more robust framework allows for the determination of larger $r_{w,crit}$ values, leading to larger but appropriately sized equipment while preserving inherent safety. However, the implementation of these more complex algorithms requires additional physicochemical parameters, which must be carefully assessed. As highlighted in the Results and Discussions section, inaccuracies in these parameters could lead to misleading or unsafe conclusions, underscoring the need for accurate input data.

4. CONCLUSIONS

Storage vessels are critical in industrial processes, particularly for containing hazardous and thermally unstable materials. Ensuring the safety of these vessels is paramount to mitigate the risks associated with runaway reactions triggered by exothermic decomposition processes. This study presented a comprehensive methodology for determining intrinsically safe vessel sizes, validated using a highly unstable mixture: 50 wt % aqueous hydroxylamine solutions.

To evaluate the influence of underlying assumptions on design outcomes, three formulations of the Frank−Kamenetskii theory of self-heating (FKT) were employed. The most comprehensive model incorporated stability and performance diagrams derived using the Varma, Morbidelli, and Wu theory of parametric sensitivity analysis (VMWT). In this framework, the Frank−Kamenetskii number δ served as a reliable reactivity index for assessing storage vessel stability. Performance diagrams further illustrated the maximum dimensionless temperature (Θ_{max}) at the critical Frank−Kamenetskii number (δ_{crit}) and a constant $\delta = 2$.

The stability and performance diagrams highlighted the influence of key dimensionless parameters − namely the dimensionless heat of reaction (B), Lewis number (Le), and reaction order (n) − on systems behavior. For large dimensionless activation energies (γ), the extended FKT formulation converged to the δ_{crit} and Θ_{max} values predicted by the canonical FKT formulation. More specifically, for $\gamma > 40$ no practical differences in the design outcomes can be retrieved. Whereas, for $\gamma > 150$ the error in both the δ_{crit} and Θ_{max} assessment is lower than 1%. In contrast, the comprehensive FKT model produced different asymptotic values depending on the governing parameters (Le, B, and n). Transitions between stable and runaway regimes were highly sensitive to input variations, with the runaway region expanding as B decreases and shrinking with decreasing Le and n. The sensitivity of the system followed the order $B > n > Le$.

Using the most refined FKT model at elevated ambient temperatures, the predicted critical radius of the storage vessel was around 12% larger than that derived from the canonical FKT. This approach also provided insights into the conservatism of the canonical FKT, demonstrating that the actual maximum temperature could be up to 4 °C lower for cylindrical geometries. The FKT framework, in all its formulations, provides a unified and interpretable index of intrinsic stability for comparing unstable substances. Higher

https://doi.org/10.1021/acs.iecr.5c00127
Ind. Eng. Chem. Res. 2025, 64, 9529−9541

$r_{w,crit}$ values for a given mixture—under the same system geometry and ambient temperature—indicate a higher level of intrinsic safety. The case study analyzed in this work shows that transitioning from 50 to 30% w/w hydroxylamine aqueous solution allows the critical storage vessel size to increase by a factor of 2.3. This approach can replace traditional comparison methods that rely on subjective risk scales with a unified, theory-based metric that quantifies both stability and safety in a single, practical indicator.

The selection of a specific refined FKT formulation for storage vessel design or intrinsic mixture stability assessment should be based on different considerations.

If a limited effort is preferred, the canonical FKT model is the most suitable choice, as it is straightforward, relies on simple mathematics, and provides conservative, safety-oriented results. Conversely, for less conservative and more optimized solutions, more advanced FKT formulations are recommended. As the model complexity increases, larger $r_{w,crit}$ values can be determined, allowing for larger inherently safe equipment that optimizes plant site utilization. For stability assessment, adopting a more refined FKT formulation provides a more accurate approximation of the reactive mixture's intrinsic behavior. However, implementing advanced models requires the use of maps or numerical approaches, as well as a detailed set of physicochemical data, which must be retrieved from literature or experimental measurements. Eventually, these additional requirements introduce further sources of uncertainties, which if not carefully managed could compromise the reliability of refined models.

Future research will focus on further relaxing FKT assumptions by incorporating natural convection effects and appropriate boundary conditions to better reflect seasonal or daily temperature fluctuations in real industrial conditions. Natural convection is expected to enhance fluid homogenization and improve heat dissipation. This, in turn, would allow for the design of larger equipment with enhanced safety margins. Variable boundary conditions will improve model fidelity to full-scale applications by accounting for seasonal and daily temperature fluctuations. However, for conservative design, considering the highest reasonable ambient temperature ensures a lower critical vessel radius, enhancing safety. Conversely, refined formulations can improve economic efficiency by optimizing vessel geometry to better suit specific applications. Additionally, future work will investigate the impact of storage time on thermal stability and evaluate design decisions within an economic optimization framework.

■ ASSOCIATED CONTENT

Supporting Information

The Supporting Information is available free of charge at https://pubs.acs.org/doi/10.1021/acs.iecr.5c00127.

The dimensionless governing values derived from the three Frank−Kamenetskii formulations (canonical, expanded, and comprehensive FKT) relevant to the design and verification of storage vessels; these values are reported for a 30% w/w hydroxylamine aqueous solution (HA30) (Table S1); the design parameters of the HA30 system as a function of the ambient temperature (Table S2) (PDF)

■ AUTHOR INFORMATION

Corresponding Author

Paolo Mocellin − *Dipartimento di Ingegneria Industriale and Dipartimento di Ingegneria Civile, Edile e Ambientale, Università degli Studi di Padova, Padova 35131, Italia;* orcid.org/0000-0002-5301-3900; Email: paolo.mocellin@unipd.it

Authors

Giuseppe Andriani − *Dipartimento di Ingegneria Industriale, Università degli Studi di Padova, Padova 35131, Italia;* orcid.org/0009-0009-4569-5006

Gianmaria Pio − *Dipartimento di Ingegneria Civile, Chimica, Ambientale e dei Materiali, Università di Bologna, Bologna 40131, Italia;* orcid.org/0000-0002-0770-1710

Ernesto Salzano − *Dipartimento di Ingegneria Civile, Chimica, Ambientale e dei Materiali, Università di Bologna, Bologna 40131, Italia;* orcid.org/0000-0002-3238-2491

Chiara Vianello − *Dipartimento di Ingegneria Industriale, Università degli Studi di Padova, Padova 35131, Italia;* orcid.org/0000-0002-5155-9061

Complete contact information is available at: https://pubs.acs.org/10.1021/acs.iecr.5c00127

Notes

The authors declare no competing financial interest.

■ ACKNOWLEDGMENTS

This research has received no external funding.

■ NOMENCLATURE

ARC	accelerating rate calorimetry
B	dimensionless heat of reaction
Bi	Biot number
C_A	dimensional concentration
C_{A0}	initial concentration of the primary reactant
$\hat{C}_p$	mixture's heat capacity per unit mass
$\tilde{C}_p$	mixture's molar heat capacity
$\mathcal{D}_{A,mix}$	mass diffusivity of the main component into the mixture
DSC	differential scanning calorimetry
E_a	activation energy
FK	Frank−Kamenetskii
FKT	Frank−Kamenetskii theory of self-heating
H	total vessel height
H_{liq}	liquid height (level)
HA30	30 % w/w aqueous solution of hydroxylamine
HA50	50% w/w aqueous solution of hydroxylamine
ISD	Inherently safer design
Le	Lewis number
n	reaction order
$k_{k\infty}$	Arrhenius pre-exponential factor
k_T	thermal conductivity
r	dimensional radial coordinate
R_g	universal gas constant
r_w	vessel radius
$r_{w,crit}$	critical vessel radius
$\mathcal{R}\vert_{T_{amb},C_{A0}}$	reaction rate evaluated at T_{amb} and C_{A0}
$S(\Theta;B)$	normalized sensitivity of Θ with respect to B
$S(\Theta;\delta)$	Normalized sensitivity of Θ with respect to δ
t	dimensional time

https://doi.org/10.1021/acs.iecr.5c00127
Ind. Eng. Chem. Res. 2025, 64, 9529−9541

T	dimensional temperature
T_{amb}	ambient temperature
T_{max}	dimensional maximum temperature
$T_{max}\|_{\delta=2}$	T_{max} evaluated at $\delta = 2$
$T_{max}\|_{\delta_{crit}}$	T_{max} evaluated at δ_{crit}
T_{onset}	onset temperature
TGA	thermogravimetric analysis
TSu	thermal screening unit
u_A	dimensionless concentration
VMWT	Varma, Morbidelli and Wu theory of parametric sensitivity analysis
α	thermal diffusivity
γ	dimensionless activation energy
δ	Frank−Kamenetskii number
δ_{crit}	critical Frank−Kamenetskii number
$\tilde{H}_r$	reaction enthalpy per mole
Θ	dimensionless temperature
Θ_{max}	dimensionless maximum temperature
$\Theta_{max}\|_{\delta=2}$	Θ_{max} evaluated at $\delta = 2$
$\Theta_{max}\|_{\delta_{crit}}$	Θ_{max} evaluated at δ_{crit}
ν_A	stoichiometric coefficient of the main reactant A
ρ	mixture's density
$\mathcal{T}$	dimensionless time
χ	conversion
Ω	dimensionless radial coordinate

REFERENCES

(1) Mocellin, P.; De Tommaso, J.; Vianello, C.; Maschio, G.; Saulnier-Bellemare, T.; Virla, L. D.; Patience, G. S. Experimental Methods in Chemical Engineering: Hazard and Operability Analysis—HAZOP. *Can. J. Chem. Eng.* **2022**, *100* (12), 3450−3469.

(2) Crowl, D. A.; Louvar, J. F. *Chemical Process Safety: Fundamentals with Applications*, 3rd ed. ed.; Pearson Education, 2011.

(3) Bassani, A.; Vianello, C.; Mocellin, P.; Dell'angelo, A.; Spigno, G.; Fabiano, B.; Maschio, G.; Manenti, F. Aprioristic Integration of Process Operations and Risk Analysis: Definition of the Weighted F&EI-Based Concept and Application to AG2S Technology. *Ind. Eng. Chem. Res.* **2023**, *62* (1), 500−510.

(4) Andriani, G.; De Liso, B.A.; Pio, G.; Salzano, E. Design of Sustainable Reactor Based on Key Performance Indicators. *Chem. Eng. Sci.* **2024**, *285*, 119591.

(5) Vianello, C.; Salzano, E.; Maschio, G. Thermal Behaviour of Peracetic Acid for the Epoxydation of Vegetable Oils in the Presence of Catalyst. *Process Saf. Environ. Prot.* **2018**, *116*, 718−726.

(6) Sivaraman, S.; Varadharajan, S. Investigative Consequence Analysis: A Case Study Research of Beirut Explosion Accident. *J. Loss Prev. Process Ind.* **2021**, *69*, 104387.

(7) Houtman, C.; Hart, P. Predicting the Autoaccelerating Hydrogen Peroxide Decomposition Rate after Mixing with Sodium Hydroxide. *Ind. Eng. Chem. Res.* **2022**, *61* (34), 12473−12481.

(8) Mannan, S.; Lees, F. *Lees' Loss Prevention in the Process Industries*, 4th ed. ed.; Butterworth-Heinemann, 2012.

(9) Andriani, G.; Mocellin, P.; Pio, G.; Vianello, C.; Salzano, E. Enhancing Safety in the Storage of Hazardous Molecules: The Case of Hydroxylamine. *J. Loss Prev. Process Ind.* **2024**, *92*, 105472.

(10) Pio, G.; Mocellin, P.; Vianello, C.; Salzano, E. A Detailed Kinetic Model for the Thermal Decomposition of Hydroxylamine. *J. Hazard. Mater.* **2021**, *416*, 125641.

(11) Vianello, C.; Salzano, E.; Broccanello, A.; Manzardo, A.; Maschio, G. Runaway Reaction for the Esterification of Acetic Anhydride with Methanol Catalyzed by Sulfuric Acid. *Ind. Eng. Chem. Res.* **2018**, *57* (12), 4195−4202.

(12) Vianello, C.; Salzano, E.; Maschio, G. Safety Parameters and Preliminary Decomposition Kinetic of Organo-Peroxy Acids in Aqueous Phase. *Chem. Eng. Trans.* **2015**, *43*, 2371−2376.

(13) Han, Y.; Shi, J.; Mao, L.; Wang, Z.; Zhang, L. Improvement of Compatibility and Mechanical Performances of PLA/PBAT Composites with Epoxidized Soybean Oil as Compatibilizer. *Ind. Eng. Chem. Res.* **2020**, *59* (50), 21779−21790.

(14) Liu, S.; Yu, D.; Chen, Y.; Shi, R.; Zhou, F.; Mu, T. High-Resolution Thermogravimetric Analysis Is Required for Evaluating the Thermal Stability of Deep Eutectic Solvents. *Ind. Eng. Chem. Res.* **2022**, *61* (38), 14347−14354.

(15) Leveneur, S. Combining Isothermal and Adiabatic Mode Experiments for Kinetic Constant Estimation: Application to the Hydrogenation of 5-(Hydroxymethyl)Furfural (5-HMF). *Ind. Eng. Chem. Res.* **2024**, *63* (10), 4362−4379.

(16) Liu, X.; Cheng, Z.; Chen, N.; Xu, F.; Liu, J.; Ni, L.; Jiang, J. Process Hazard Assessment and Exothermic Mechanism of Propylene Glycol Butyl Ether Synthesis from Propylene Oxide. *Ind. Eng. Chem. Res.* **2024**, *63* (12), 5097−5112.

(17) Lakhe, P.; Kulhanek, D. L.; Zhao, X.; Papadaki, M. I.; Majumder, M.; Green, M. J. Graphene Oxide Synthesis: Reaction Calorimetry and Safety. *Ind. Eng. Chem. Res.* **2020**, *59* (19), 9004−9014.

(18) Andriani, G.; Pio, G.; Salzano, E.; Vianello, C.; Mocellin, P. Evaluating the Thermal Stability of Chemicals and Systems: A Review. *Can. J. Chem. Eng.* **2025**, *103*, 42.

(19) Brown, M. E.; Gallagher, P. K. *Handbook of Thermal Analysis and Calorimetry*, 1st ed.; Elsevier, 2003, Vol. 5.

(20) Frank-Kamenetskii, D. A. *Diffusion and Heat Exchange in Chemical Kinetics*, 1st ed.; Princeton University Press, 1955.

(21) Restuccia, F.; Huang, X.; Rein, G. Self-Ignition of Natural Fuels: Can Wildfires of Carbon-Rich Soil Start by Self-Heating? *Fire Saf. J.* **2017**, *91*, 828−834.

(22) Hurley, M. J. *SFPE Handbook Af Fire Protection Engineering*, 5th ed. ed.; Springer, 2016.

(23) Luo, Q.; Liang, D.; Shen, H. Evaluation of Self-Heating and Spontaneous Combustion Risk of Biomass and Fishmeal with Thermal Analysis (DSC-TG) and Self-Heating Substances Test Experiments. *Thermochim. Acta* **2016**, *635*, 1−7.

(24) Zhang, J.; Zhang, L.; Men, C.; Ren, M.; Zhang, H.; Lu, J. Ignition of Supercritical Hydrothermal Flames in Co-Flow Jets. *J. Supercrit. Fluids* **2022**, *188*, 105683.

(25) Boddington, T.; Feng, C.; Gray, P. Thermal Explosions, Criticality and the Disappearance of Criticality in Systems with Distributed Temperatures. Arbitrary Biot Number and General Reaction-Rate Laws. *Proc. R. Soc. London, A* **1983**, *390* (1799), 247−264.

(26) Maestri, F.; Rota, R. Kinetic-Free Safe Operation of Fine Chemical Runaway Reactions: A General Criterion. *Ind. Eng. Chem. Res.* **2016**, *55* (4), 925−933.

(27) Yang, L.; Sheng, J. J. Feasibility of Using the Frank-Kamenetskii Theory to Predict the Spontaneous Ignition of the Crude Oil-Sand Mixture. *Energy Fuels* **2019**, *33* (6), 4816−4825.

(28) Varma, A.; Morbidelli, M.; Wu, H. *Parametric Sensitivity in Chemical Systems*, 1st ed.; Cambridge University Press, 1999.

(29) Lengyel, I.; West, D. H. Numerical Bifurcation Analysis of Large-Scale Detailed Kinetics Mechanisms. *Curr. Opin. Chem. Eng.* **2018**, *21*, 41−47.

(30) Restuccia, F.; Fernandez-Anez, N.; Rein, G. Experimental Measurement of Particle Size Effects on the Self-Heating Ignition of Biomass Piles: Homogeneous Samples of Dust and Pellets. *Fuel* **2019**, *256*, 115838.

(31) He, X.; Hu, Z.; Restuccia, F.; Fang, J.; Rein, G. Experimental Study of the Effect of the State of Charge on Self-Heating Ignition of Large Ensembles of Lithium-Ion Batteries in Storage. *Appl. Therm. Eng.* **2022**, *212*, 118621.

(32) Stoessel, F. *Thermal Safety of Chemical Processes*, 2nd ed. ed.; Wiley-VCH, 2020.

(33) Wang, Q.; Rogers, W. J.; Mannan, M. S. Thermal Risk Assessment and Rankings for Reaction Hazards in Process Safety. *J. Therm. Anal. Calorim.* **2009**, *98* (1), 225−233.

https://doi.org/10.1021/acs.iecr.5c00127
Ind. Eng. Chem. Res. 2025, 64, 9529−9541

(34) Paltrinieri, N.; Khan, F. *Dynamic Risk Analysis in the Chemical and Petroleum Industry*, 1st ed.; Elsevier, 2016.
(35) De Liso, B. A.; Pio, G.; Salzano, E. Multicriteria Approach to Assess the Fire Behaviour of Polymers in Electrochemical Energy Storage. *J. Loss Prev. Process Ind.* **2025**, *94*, 105541.
(36) Maestri, F.; Rota, R. Kinetic-Free Safe Optimization of a Semibatch Runaway Reaction: Nitration of 4-Chloro Benzotrifluoride. *Ind. Eng. Chem. Res.* **2016**, *55* (50), 12786−12794.
(37) Kletz, T. A. Inherently Safer Design - Its Scope and Future. *Process Saf. Environ. Prot.* **2003**, *81* (6), 401−405.
(38) Ortiz-Espinoza, A. P.; Jiménez-Gutiérrez, A.; El-Halwagi, M. M. Including Inherent Safety in the Design of Chemical Processes. *Ind. Eng. Chem. Res.* **2017**, *56* (49), 14507−14517.
(39) Guo, Z.; Chen, L.; Chen, W. Development of Adiabatic Criterion for Runaway Detection and Safe Operating Condition Designing in Semibatch Reactors. *Ind. Eng. Chem. Res.* **2017**, *56* (50), 14771−14780.
(40) Andriani, G.; Mocellin, P.; Pio, G.; Salzano, E.; Vianello, C. Hydroxylamine vs. Hydrogen Peroxide: A Comparative Study on Storage Stability. *Chem. Eng. Trans.* **2024**, *111*, 277−282.
(41) *Ullmanns Encyclopedia of Industrial Chemistry*. 7th ed.ed.; Wiley-VCH, 2011.
(42) Chen, L.; Li, X.; Zhang, J.; Fang, J.; Huang, Y.; Wang, P.; Ma, J. Production of Hydroxyl Radical via the Activation of Hydrogen Peroxide by Hydroxylamine. *Environ. Sci. Technol.* **2015**, *49* (17), 10373−10379.
(43) He, X.; Restuccia, F.; Zhang, Y.; Hu, Z.; Huang, X.; Fang, J.; Rein, G. Experimental Study of Self-Heating Ignition of Lithium-Ion Batteries During Storage: Effect of the Number of Cells. *Fire Technol.* **2020**, *56* (6), 2649−2669.
(44) Babrauskas, V. *Ignition Handbook: principles and Applications to Fire Safety Engineering, Fire Investigation, Risk Management and Forensic Science*, 2nd ed. ed.; Fire Science Publishers, 2014.
(45) Chen, X. D.; Sidhu, H.; Nelson, M. A Linear Relationship between Dimensionless Crossing-Point-Temperature and Frank-Kamenetskii Reactivity Parameter in Self-Heating Test at Infinite Biot Number for Slab Geometry. *Fire Saf. J.* **2013**, *61*, 138−143.
(46) Restuccia, F.; Mašek, O.; Hadden, R. M.; Rein, G. Quantifying Self-Heating Ignition of Biochar as a Function of Feedstock and the Pyrolysis Reactor Temperature. *Fuel* **2019**, *236*, 201−213.
(47) Restuccia, F.; Ptak, N.; Rein, G. Self-Heating Behavior and Ignition of Shale Rock. *Combust. Flame* **2017**, *176*, 213−219.
(48) Harley, C.; Momoniat, E. Alternate Derivation of the Critical Value of the Frank-Kamenetskii Parameter in Cylindrical Geometry. *J. Nonlinear Math. Phys.* **2008**, *15*, 69−76.
(49) Chambré, P. L. On the Solution of the Poisson-Boltzmann Equation with Application to the Theory of Thermal Explosions. *J. Chem. Phys.* **1952**, *20* (11), 1795−1797.
(50) Morbidelli, M.; Varma, A. Parametric Sensitivity and Runaway in Fixed-Bed Catalytic Reactors. *Chem. Eng. Sci.* **1986**, *41* (4), 1063−1071.
(51) Morbidelli, M.; Varma, A. A Generalized Criterion for Parametric Sensitivity: Application to Thermal Explosion Theory. *Chem. Eng. Sci.* **1988**, *43* (I), 91−102.
(52) Haaker, M. P. R.; Verheijen, P. J. T. Local and Global Sensitivity Analysis for a Reactor Design with Parameter Uncertainty. *Chem. Eng. Res. Des.* **2004**, *82* (5), 591−598.
(53) Saltelli, A.; Ratto, M.; Tarantola, S.; Campolongo, F. Sensitivity Analysis for Chemical Models. *Chem. Rev.* **2005**, *105*, 2811−2827.
(54) Jiang, J.; Jiang, J.; Pan, Y.; Wang, R.; Tang, P. Investigation on Thermal Runaway in Batch Reactors by Parametric Sensitivity Analysis. *Chem. Eng. Technol.* **2011**, *34* (9), 1521−1528.
(55) Kummer, A.; Varga, T. What Do We Know Already about Reactor Runaway? − A Review. *Process Saf. Environ. Prot.* **2021**, *147*, 460−476.
(56) Zang, N.; Qian, X. M.; Shu, C. M.; Wu, D. Parametric Sensitivity Analysis for Thermal Runaway in Semi-Batch Reactors: Application to Cyclohexanone Peroxide Reactions. *J. Loss Prev. Process Ind.* **2021**, *70*, 104436.
(57) American Petroleum Institute. *API Standard 650: welded Tanks for Oil Storage*, 11th ed. ed.; American Petroleum Institute, 2007.
(58) Andriani, G.; Pio, G.; Vianello, C.; Mocellin, P.; Salzano, E. Safety Parameters and Stability Diagram of Hydroxylamine Hydrochloride and Sulphate. *Chem. Eng. J.* **2024**, *482*, 148894.
(59) Picioreanu, C.; Loosdrecht, M. C. M. V.; Heijnen, J. J. Modelling the Effect of Oxygen Concentration on Nitrite Accumulation in a Biofilm Airlift Suspension Reactor. *Water Sci. Technol.* **1997**, *36* (1), 147−156.
(60) Vianello, C.; Salzano, E.; Maschio, G. Kinetics and Safety Analysis of Peracetic Acid. *Chem. Eng. Trans.* **2016**, *48*, 559−564.

https://doi.org/10.1021/acs.iecr.5c00127
Ind. Eng. Chem. Res. 2025, 64, 9529−9541